

Laser-induced photoacoustics influenced by single-cycle terahertz radiation

Benjamin Clough, Jingle Liu, and X.-C. Zhang*

Center for Terahertz Research, Rensselaer Polytechnic Institute, Troy, New York 12180, USA

*Corresponding author: zhangxc@rpi.edu

Received June 1, 2010; revised September 8, 2010; accepted September 17, 2010;

posted September 29, 2010 (Doc. ID 129168); published October 19, 2010

Laser-induced plasma acoustic waves are enhanced under the illumination of single-cycle terahertz (THz) radiation, making THz-enhanced acoustics (TEA) a useful method for THz wave detection. During a single-cycle THz pulse with its peak field of 100 kV/cm, a pressure enhancement of 10% is observed throughout the acoustic spectrum up to 140 kHz, and the TEA signal is found to increase linearly with THz wave intensity. By using dual-color laser excitation to manipulate free electron drift, it is possible to modulate the enhanced acoustic signal and recover a coherent THz time-domain waveform by simply “listening” to the plasma. © 2010 Optical Society of America
OCIS codes: 040.2235, 140.3440, 280.3375, 350.5400, 120.0280.

Laser-induced plasma continues to gain interest because of its increasing number of scientific and technological applications in photoionization [1], high-harmonic generation [2], laser-induced breakdown spectroscopy [3], spark-induced breakdown spectroscopy [4], and the generation and detection of broadband terahertz (THz) pulses [5–7]. Since the advent of millijoule, femtosecond pulsed lasers, laser-induced plasma has been employed to study the interaction between light and matter and reveal ultrafast dynamics of solids, liquids, and gases [8,9]. However, the respective fields of THz photonics and photoacoustics have, for the most part, remained nonoverlapping. Laser-induced plasma acoustic dynamics under the influence of single-cycle electromagnetic radiation and its underlying physical mechanism currently remain unexplored. The study presented in this Letter will provide information relevant to THz wave detection that may also be useful for other plasma applications, such as laser plasma shock wave evolution, propulsion, plasma heating, and plasma diagnostics.

In the experiment illustrated in Fig. 1(a), either a single-color (800 nm) or a dual-color (800 nm + 400 nm) laser pulse was focused in air to produce an acoustic pulse. The case of single-color laser excitation is discussed first. The total laser intensity at the focus was 10^{13} – 10^{14} W/cm². Under illumination of an intense femtosecond laser pulse, photoionization of the molecules takes place in the subpicosecond time scale. The laser field increases free electron temperature, T_e , to 10^4 – 10^5 K, while neighboring molecules or ions have a much lower temperature, T_m [10]. In the following 10^{-8} – 10^{-9} s, T_m is gradually increased through energy transfer from collisions between hot electrons and their surrounding air molecules until thermal equilibrium is achieved [11,12]. This rise in localized gas temperature produces a shock wave that persists for a short distance [13] before relaxing into an acoustic wave [14].

The waveform of the acoustic pulse was measured with a broadband microphone (G.R.A.S. 40DP). A single-cycle THz pulse with peak field of approximately 100 kV/cm, generated using the tilted pulse front optical rectification technique in LiNiO₃ [15], was spatially overlapped with the optical pulse (800 nm, 65 fs, 110 μJ pulse energy, 1 kHz repetition rate). When the time delay

between the THz pulse and the optical pulse, t_D in Fig. 1(a), was negative (optical pulse preceding THz pulse), the acoustic pressure wave was observed to be enhanced by the THz field. Figure 1(b) shows the measured acoustic waveforms with and without the 100 kV/cm THz field incident on the plasma. A 10% amplitude enhancement of the sound pressure in the entire waveform was observed.

The inset of Fig. 1(b) shows the THz-induced pressure enhancement in the frequency domain after Fourier transformation of the single-pulse waveforms. The

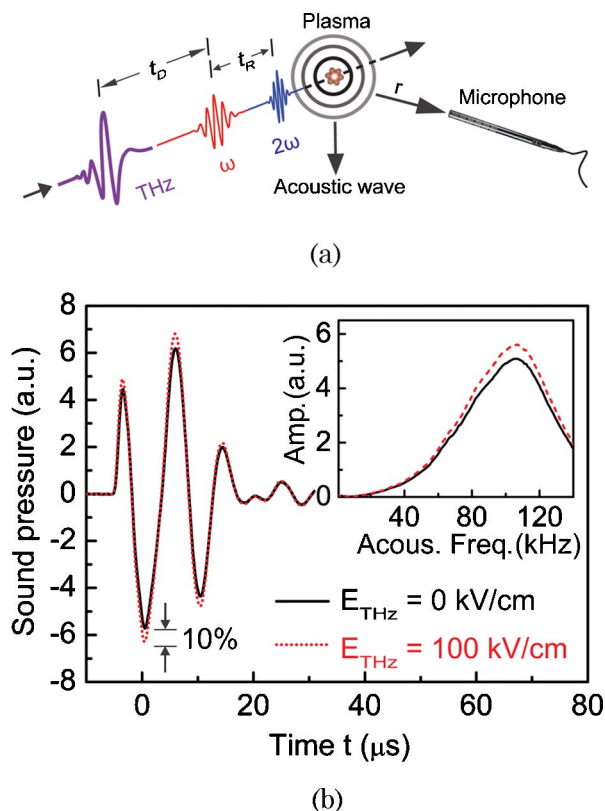


Fig. 1. (Color online) (a) Experimental schematic for the TEA using single-color or dual-color femtosecond laser excitation. (b) Single photoacoustic waveforms measured at a 5 mm distance with (red dashed curve) and without (black solid curve) a 100 kV/cm THz field. The inset shows acoustic spectra.

acoustic enhancement ratio remains nearly 10% over the entire bandwidth of the microphone (up to 140 kHz). A pair of wire grid polarizers was used to determine the acoustic enhancement dependence on THz intensity. A lock-in amplifier measured the acoustic signal at 100 kHz, using the 100th harmonic of the laser repetition rate (1 kHz). The inset of Fig. 2 shows the acoustic enhancement at 100 kHz for different THz intensities. Good agreement between the measurement and the linear fit shows that the enhanced acoustic pressure is linearly dependent on incident THz wave intensity.

To study laser-induced photoacoustic dynamics under single-cycle THz radiation, the acoustic signal at 100 kHz was measured by varying the time delay t_D . The results are shown as the solid curve in Fig. 2. In region I, the THz pulse leads the optical pulse in time and there is no acoustic enhancement, because there is no interaction between the THz pulse and the plasma; however, when the field of the THz pulse begins to interact with the plasma, a sharp rise in the acoustic signal is observed, with the period of rising time comparable to the width of a single-cycle THz pulse. In region II, following the rise, a slow decay of the acoustic signal of the order of nanoseconds is observed and agrees with the temporal profile of the electron density decay due to electron-ion recombination [16].

The enhancement of the acoustic pressure is attributed to electron heating in the THz field and subsequent increased temperature of air molecules through electron-molecule collision. Since the electron relaxation time, τ , at atmospheric pressure is small in comparison to the THz pulse duration [17], the pressure enhancement Δp can be approximated as $\frac{e^2 \tau}{m_e} \int_{t_D}^{\infty} E_{\text{THz}}(t')^2 dt'$ [18]. The quadratic dependence on the THz field is also consistent with the linear fit in the inset of Fig. 2. The calculated acoustic pressure in Fig. 2 shows enhancement at a certain frequency (e.g., $f = 100$ kHz) when using the equation above as compared with the experimental measurement.

In addition to the case of single-color laser plasma excitation, TEA has also demonstrated the ability to coherently detect THz pulses using a dual-color laser-produced plasma. By using the superposition of two optical pulses (800 nm ω and 400 nm 2ω) linearly polarized in the same

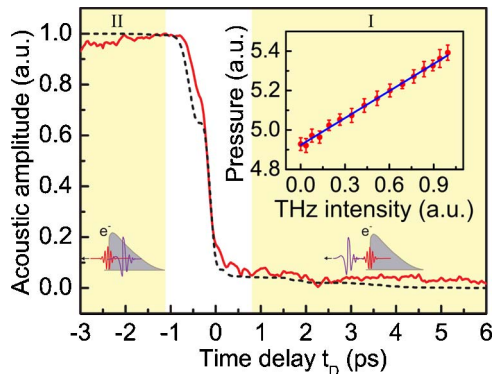
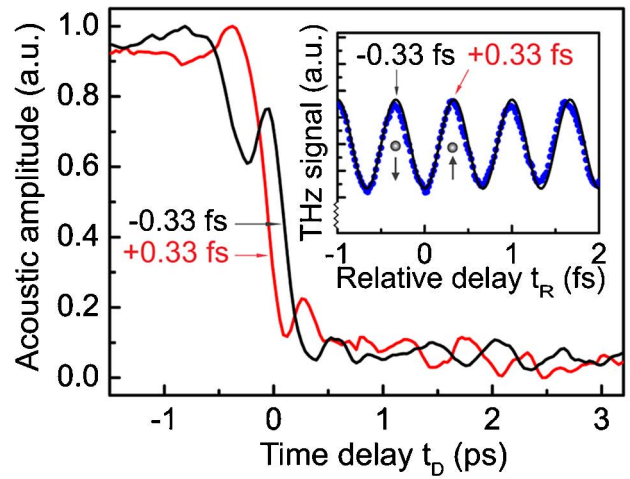
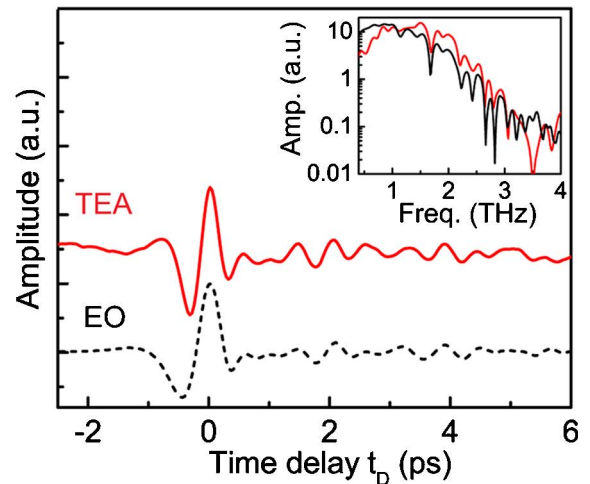


Fig. 2. (Color online) Measured TEA signal at 100 kHz as a function of t_D . Region I, THz pulse leads the optical pulse in time; region II, THz pulse trails the optical pulse in time. The dashed curve is the calculated TEA signal. Inset shows the acoustic signal at 100 kHz for different THz intensities incident on single-color laser-induced plasma and a linear fit.

direction, the net electron drift inside the plasma can be controlled by changing the relative phase between the pulses, t_R [19]. The symmetry of drift velocity can be determined by the THz wave generation from laser-induced plasma as described in [20], and results are shown in the inset of Fig. 3(a). The quasi-unipolar net drift is in the parallel direction at a phase of $+0.33$ fs, while the quasi-unipolar net electron drift is in the antiparallel direction at the phase of -0.33 fs [21,22]. When a THz field is introduced for each of these relative optical phase delays between ω and 2ω , the electrons that experience the THz field are either slightly accelerated or decelerated depending on whether the THz field is antiparallel or parallel to the direction of the electron net drift. Scanning the delay between the THz and optical pulses t_D for a given relative delay t_R of -0.33 fs and $+0.33$ fs between the ω and 2ω pulses, the rising enhancement curves for opposite net electron drift directions are obtained. The



(a)



(b)

Fig. 3. (Color online) (a) Time-resolved TEA signals obtained for $t_R = 0.33$ fs and $t_R = +0.33$ fs. The inset shows the measured THz wave generation from dual-color laser-induced plasma at different t_R (no external THz field present). (b) THz time-domain waveforms obtained using the THz-enhanced acoustics method and EO sampling. The inset shows corresponding THz spectra.

results are plotted in Fig. 3(a). In both cases, there is acoustic wave enhancement, which results from THz-field-induced electron heating and increased electron-molecule collision. However, under parallel and antiparallel conditions, the free electrons will either be decelerated or accelerated along the direction of the THz field, contributing to the overall acoustic emission. By subtracting the TEA curves for these respective phases, both “background” acoustic emission from the dual-color plasma and the second-order heating term [$\sim E_{\text{THz}}(t)^2$] are canceled, since these are symmetric for the dual-color ionization. This leaves only the change in acoustic emission from electron momentum change by the THz field before the first collision event [$E_{\text{THz}}(t)$ first-order term], after which the electron drift is randomized. Therefore, $\Delta p(-0.33 \text{ fs}) - \Delta p(+0.33 \text{ fs}) \propto E_{\text{THz}}(t)$ [23]. It is also possible to recover the THz signal if, for one case, we used a phase delay of 0 fs between ω and 2ω that produced a symmetric electron drift, and in the other produced a case of asymmetry (parallel or antiparallel). We chose to use parallel and antiparallel delays because this gives a factor of 2 in the pressure contribution from the THz signal. To verify the equation above, the measured THz time-domain waveforms and spectra using this method are compared with conventional electro-optic (EO) sampling. From Fig. 3(b) and its inset, it is apparent that these methods produce similar results and the locations of water absorption lines are consistent with previously reported data [24].

In conclusion, it has been experimentally demonstrated that the acoustic waves from a laser-induced plasma can be enhanced under single-cycle THz radiation. The TEA emission varies linearly with the THz intensity incident on the plasma, and approximately 10% acoustic enhancement is observed throughout the 140 kHz bandwidth of the broadband microphone signal. TEA can be attributed to THz plasma heating, through energy transfer from the THz wave into translational motion of the gas molecules. Potential applications of these experimental findings include a promising method for coherent THz wave detection at remote distances, and as a diagnostic tool for dynamic plasma interactions with electromagnetic radiation.

This material is based upon work supported by the National Science Foundation (NSF) under grant no. 0333314. The authors thank Professor Ning Xiang for valuable discussions and technical assistance, and we gratefully acknowledge support from the NSF, the Office

of Naval Research (ONR), the Defense Threat Reduction Agency, and the Department of Homeland Security through the DHS-ALERT Center under award no. 2008-ST-061-ED0001.

References

1. P. B. Corkum, *Phys. Rev. Lett.* **71**, 1994 (1993).
2. A. L'Huillier and P. Balcou, *Phys. Rev. Lett.* **70**, 774 (1993).
3. D. A. Rusak, B. C. Castle, B. W. Smith, and J. D. Winefordner, *Crit. Rev. Anal. Chem.* **27**, 257 (1997).
4. Y. Ikeda, A. Moon, and M. Kaneko, *Appl. Opt.* **49**, C95 (2010).
5. H. Hamster, A. Sullivan, S. Gordon, W. White, and R. W. Falcone, *Phys. Rev. Lett.* **71**, 2725 (1993).
6. D. J. Cook and R. M. Hochstrasser, *Opt. Lett.* **25**, 1210 (2000).
7. M. Kress, T. Löffler, S. Eden, M. Thomson, and H. G. Roskos, *Opt. Lett.* **29**, 1120 (2004).
8. M. Tonouchi, *Nat. Photon.* **1**, 97 (2007).
9. G. A. West, J. J. Barrett, D. R. Siebert, and K. V. Reddy, *Rev. Sci. Instrum.* **54**, 797 (1983).
10. G. N. Gibson, R. R. Freeman, and T. J. McIlrath, *Phys. Rev. Lett.* **67**, 1230 (1991).
11. J. Yu, D. Mondelain, J. Kasparian, E. Salmon, S. Geffroy, C. Favre, V. Boutou, and J.-P. Wolf, *Appl. Opt.* **42**, 7117 (2003).
12. A. Filin, R. Compton, D. A. Romanov, and R. J. Levis, *Phys. Rev. Lett.* **102**, 155004 (2009).
13. X.-W. Ni, B. Zou, J.-P. Chen, B.-M. Bian, Z.-H. Shen, and J. Lu, *Acta Phys. Sin.* **7**, 143 (1998).
14. H. Sobral, M. Villagran-Muniz, R. Navarro-Gonzalez, and A. C. Raga, *Appl. Phys. Lett.* **77**, 3158 (2000).
15. J. Hebling, K.-L. Yeh, M. C. Hoffmann, B. Bartal, and K. A. Nelson, *J. Opt. Soc. Am. B* **25**, B6 (2008).
16. S. Tzortzakis, B. Prade, M. Franco, and A. Mysyrowicz, *Opt. Commun.* **181**, 123 (2000).
17. M. Mlejnek, E. M. Wright, and J. V. Moloney, *Phys. Rev. E* **58**, 4903 (1998).
18. J. Liu and X. C. Zhang, *Phys. Rev. Lett.* **103**, 235002 (2009).
19. K.-Y. Kim, J. H. Glowina, A. J. Taylor, and G. Rodriguez, *Opt. Express* **15**, 4577 (2007).
20. J. Dai, N. Karpowicz, and X. C. Zhang, *Phys. Rev. Lett.* **103**, 023001 (2009).
21. D. Schumacher, F. Weihe, H. Muller, and P. Bucksbaum, *Phys. Rev. Lett.* **73**, 1344 (1994).
22. N. Karpowicz and X. C. Zhang, *Phys. Rev. Lett.* **102**, 093001 (2009).
23. J. Liu, J. Dai, S. L. Chin, and X. C. Zhang, *Nat. Photon.* **4**, 627 (2010).
24. M. V. Exter, C. Fattinger, and D. Grischkowsky, *Opt. Lett.* **14**, 1128 (1989).